

Talk presented at the APS Division of Particles and Fields Meeting (DPF 2017)  
July 31-August 4, 2017, Fermilab. C170731

# Automated proton track identification in MicroBooNE using gradient boosted decision trees

**Katherine Woodruff**

on behalf of the MicroBooNE collaboration

*Physics Department, New Mexico State University  
Las Cruces, NM 88003*

E-mail: [kwoodruf@nmsu.edu](mailto:kwoodruf@nmsu.edu)

**Abstract.** MicroBooNE is a liquid argon time projection chamber (LArTPC) neutrino experiment that is currently running in the Booster Neutrino Beam at Fermilab. LArTPC technology allows for high-resolution, three-dimensional representations of neutrino interactions. A wide variety of software tools for automated reconstruction and selection of particle tracks in LArTPCs are actively being developed. Short, isolated proton tracks, the signal for low-momentum-transfer neutral current (NC) elastic events, are easily hidden in a large cosmic background. Detecting these low-energy tracks will allow us to probe interesting regions of the proton's spin structure. An effective method for selecting NC elastic events is to combine a highly efficient track reconstruction algorithm to find all candidate tracks with highly accurate particle identification using a machine learning algorithm. We present our work on particle track classification using gradient tree boosting software (XGBoost) and the performance on simulated neutrino data.

## 1. Introduction

The three up and down valence quarks in the nucleon only account for a small percent of its mass. Gluons that bind the valence quarks split into quark-antiquark pairs of up, down, and strange flavor. This sea of quarks and gluons carries the remainder of the nucleon mass. The structure of the quark-gluon sea and how its elements combine with the valence quarks to give the nucleon its measured structure is not precisely known.

The net spin of the proton comes from a combination of the spin and orbital momentum of the quarks and gluons. The net contribution from the spin of strange quarks and antiquarks,  $\Delta s$ , is defined as

$$\Delta s = \int_0^1 \Delta s(x) dx$$

$$\Delta s(x) = \sum_{r=\pm 1} r [s^{(r)}(x) + \bar{s}^{(r)}(x)],$$

where  $s(\bar{s})$  is the spin-dependent parton distribution function of the strange (anti)quark,  $r$  is the helicity of the quark relative to the proton helicity and  $x$  is the Bjorken scaling variable [1]. In the static quark model this value is zero.

In the 1980s the European Muon Collaboration [2] and several subsequent experiments found that the Ellis-Jaffe Sum Rule was violated in polarized, charged-lepton, inclusive, deep inelastic scattering (DIS). The Ellis-Jaffe sum rule [3] assumes that SU(3) flavor symmetry is valid and that  $\Delta s = 0$ . For the results to be consistent with exact SU(3) flavor symmetry,  $\Delta s$  must be *negative*. Follow-up measurements using semi-inclusive deep inelastic scattering have been consistent with  $\Delta s = 0$ , but these determinations of  $\Delta s$  are highly dependent on the fragmentation functions used [4].

An independent determination of  $\Delta s$  can be made using neutral-current (NC) elastic neutrino-proton scattering. The NC elastic cross section depends directly on  $\Delta s$  and no assumptions about SU(3) flavor symmetry or fragmentation functions are needed.

Previous measurements using elastic neutron-proton scattering [5, 6, 7] have been able to resolve final state protons down to a kinetic energy of  $T \sim 240$  MeV which corresponds to a momentum transfer of  $Q^2 = 0.45$  GeV<sup>2</sup>. These measurements also found  $\Delta s < 0$ , but the results are highly dependent on the choice of the axial form factor  $Q^2$  dependence. To extract  $\Delta s$ ,  $G_A^s$  must be extrapolated to  $Q^2 = 0$ . Detecting events with lower momentum transfer would lessen the dependence on the choice of the model.

Global fits to electron-proton and neutrino-proton elastic scattering data have found  $\Delta s = -0.30 \pm 0.42$  [8]. Based on data from a simulation of the MicroBooNE detector and the BNB beam, the uncertainty on the global fit to  $\Delta s$  is estimated to decrease by a factor of ten when including MicroBooNE data.

## 2. Elastic neutrino-proton scattering

The elastic lepton-nucleon scattering cross section depends on the axial, electric, and magnetic form factors which represent the finite structure of the nucleon. The axial form factor,  $G_A$ , represents the spin structure, and the electric and magnetic form factors,  $G_E$  and  $G_M$ , represent the electric and magnetic structure, respectively.

### 2.1. Neutral-current elastic scattering

The NC elastic neutrino-proton cross section [1] can be written as

$$\begin{aligned} \left( \frac{d\sigma}{dQ^2} \right)_\nu^{NC} &= \frac{G_F^2}{2\pi} \left[ \frac{1}{2} y^2 (G_M^{NC})^2 \right. \\ &+ \left( 1 - y - \frac{M}{2E} y \right) \frac{(G_E^{NC})^2 + \frac{E}{2M} y (G_M^{NC})^2}{1 + \frac{E}{2M} y} \\ &+ \left( \frac{1}{2} y^2 + 1 - y + \frac{M}{2E} y \right) (G_A^{NC})^2 \\ &\left. + 2y \left( 1 - \frac{1}{2} y \right) G_M^{NC} G_A^{NC} \right], \end{aligned}$$

where  $G_F$  is the Fermi constant,  $M$  is the mass of the nucleon,  $E$  is the neutrino energy,  $Q^2$  is the momentum transfer, and  $y$  is the fractional energy loss of the incoming lepton.

The neutral-current form factors,  $G_A^{NC}$ ,  $G_E^{NC}$ , and  $G_M^{NC}$ , are functions of  $Q^2$  and can all be

written as a linear combination of the individual quark contributions

$$\begin{aligned}
G_{E,M}^{NC,p}(Q^2) &= \left(1 - \frac{8}{3}\sin^2\theta_W\right) G_{E,M}^u(Q^2) \\
&\quad + \left(-1 + \frac{4}{3}\sin^2\theta_W\right) G_{E,M}^d(Q^2) \\
&\quad + \left(-1 + \frac{4}{3}\sin^2\theta_W\right) G_{E,M}^s(Q^2) \\
G_A^{NC,p}(Q^2) &= \frac{1}{2} \left[-G_A^u(Q^2) + G_A^d(Q^2) + G_A^s(Q^2)\right].
\end{aligned}$$

The up, down, and strange quark contributions to the electric and magnetic form factors of the proton have been determined in a world-wide measurement program of elastic electron-proton scattering using hydrogen targets and quasi-elastic electron-nucleon scattering using light nuclear targets (specifically deuterium and helium) [9, 10].

We plan to measure the ratio of the neutral-current elastic cross section to the charged-current elastic cross section. The charged-current (CC) elastic cross section does not depend on  $\Delta s$ , but it is better known than the NC elastic cross section. Taking the ratio of the two cross sections reduces systematic uncertainty on our measurement due to the beam flux, detector efficiency, and nuclear effects and final state interactions in argon nuclei.

### 2.2. Axial form factor

At the limit when the momentum transfer ( $Q^2$ ) goes to zero, the quark contributions to the axial form factor become the net contribution of individual quark spin to the proton spin,

$$G_A^q(Q^2 = 0) = \Delta q \quad (q = u, d, s),$$

so that

$$G_A^{NC}(Q^2 = 0) = \frac{1}{2}(-\Delta u + \Delta d + \Delta s).$$

The difference of the up and down spin contributions,  $\Delta u - \Delta d$ , is proportional to the axial vector coupling constant  $g_A$  measured in hyperon  $\beta$  decay [11], therefore a measurement of  $G_A^{NC}$  can determine  $\Delta s$ .

### 2.3. Experimental measurement

The final state of an NC elastic neutrino-proton interaction consists of a neutrino and a proton. Since it isn't possible to detect the outgoing neutrino, the signal is a single proton track. In order to extrapolate the axial form factor to zero, we need to detect very low energy protons. The kinematics of the interaction are determined entirely by the proton kinetic energy,  $T_P$ ,

$$Q^2 = 2T_P M.$$

We estimate that MicroBooNE can detect NC elastic events down to a minimum of  $Q^2 \sim 0.08$  GeV<sup>2</sup>. The momentum transfer is determined by the kinetic energy of the proton in NC elastic interactions. MicroBooNE can detect protons with a track length of at least 1.5 cm which corresponds to a kinetic energy of  $\sim 40$  MeV in liquid argon giving  $Q^2 \sim 0.08$  GeV<sup>2</sup>.

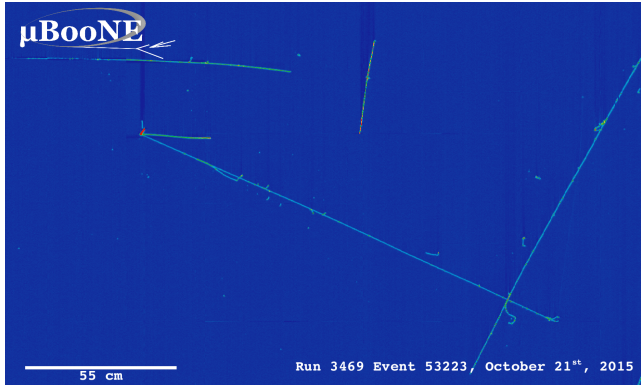


**Figure 1.** A neutrino interaction in the MicroBooNE detector. This is a candidate charged-current, muon-neutrino event with a long muon track, a charged pion track, and a short proton track coming from the interaction vertex.

### 3. MicroBooNE

The MicroBooNE detector [12] is a liquid-argon time projection chamber (TPC) located in the Booster Neutrino Beam at Fermilab. MicroBooNE is a high-resolution detector designed to be able to accurately identify low-energy neutrino interactions. It began taking data in October of 2015. Figure 1 shows an example neutrino interaction in MicroBooNE.

The MicroBooNE TPC [12] has an active mass of 89 tons of liquid argon. It is 10 meters long in the beam direction, 2.3 meters tall, and 2.5 meters in the electron drift direction. It takes 2.3 ms for electrons to drift across the full width of the TPC at the operating electric field of 273 V/cm. Events are read out on three anode wire planes with 3 mm spacing. In addition to the TPC, there is a light collection system which consists of 32 8-inch PMTs with nanosecond timing resolution. The PMTs determine the initial time of the interaction to help with cosmic rejection. In order for an event to be read out, there must be an optical signal within a 23  $\mu$ s window around the BNB spill.

The data from each neutrino event in MicroBooNE can be visualized as a set of three high resolution images (one from each anode plane). Each image has approximately 20 million pixels (3,000 wires by 9,600 time ticks). It takes 30 MB of disk space to store one MicroBooNE event.

#### 3.1. Events in MicroBooNE

An *event* in MicroBooNE has 4.8 ms of TPC readout information. This includes the 2.3 ms of time after the optical trigger to allow electrons to drift the entire distance and time before and after the 2.3 ms time frame to help identify cosmic background. In Fig. 1, the X-axis corresponds to wire number and the Y-axis corresponds to time tick. The dark blue background corresponds to no signal on the wire, and the colored pixels correspond to charge deposited on the wire. The color or intensity of the pixel corresponds to the amount of energy deposited in the TPC.

### 4. Automated event selection

MicroBooNE is close to the surface of the Earth, which results in a large cosmic ray background. Each triggered event is read out for 4.8 ms (approximately twice the electron drift time), and there are an average of twelve cosmic muon tracks per readout frame [13]. This can be seen in the bottom image in Fig. 2. In addition, there are approximately five times as many event triggers caused by cosmic rays coincident with the BNB spill than actual neutrino interactions. During MicroBooNE's three year run, we expect to have  $\sim 200,000$  neutrino interactions and  $\sim 1,000,000$  cosmic interactions. This means that automated neutrino event reconstruction and identification algorithms are required. These algorithms are currently being developed for liquid argon TPCs.

Because each event in MicroBooNE contains around 60 million pixels, we need to reduce the amount of data without removing a lot of information before trying to classify the event. We do

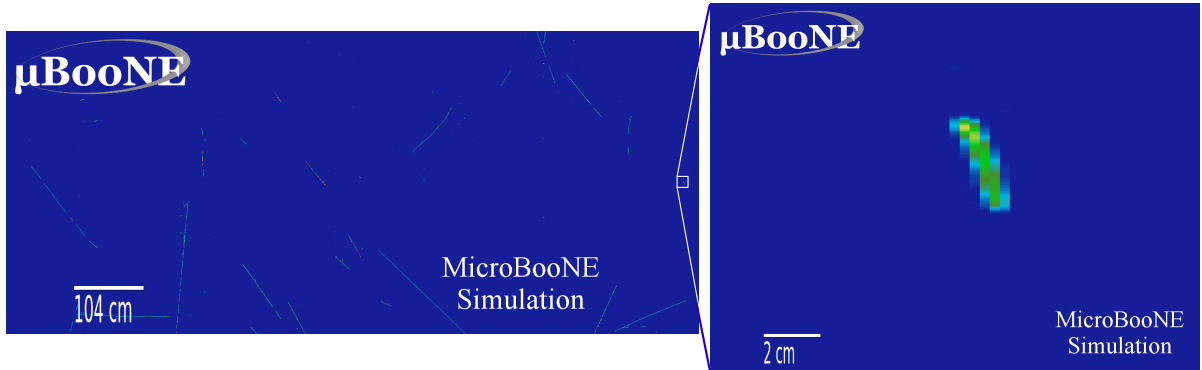


**Figure 2.** 2D event display of a simulated neutral-current elastic event in MicroBooNE that was successfully classified as a proton. The top image is a close-up event display of the simulated proton track. The bottom image shows the side view of the entire MicroBooNE TPC. All of the additional tracks are from cosmic rays.

this by grouping the one-dimensional hits on the wires into two-dimensional lines on the planes and then into three-dimensional track objects in the TPC.

#### 4.1. Track reconstruction in LArSoft

Track reconstruction is handled in the Liquid Argon Software framework (LArSoft) [14]. The three main stages of reconstruction in LArSoft are hit finding, track finding, and event identification.

One-dimensional hits are found by fitting Gaussian functions to noise-filtered [15] waveforms that are read out from the anode wires in the TPC. This is done for all of the wires on all three of the planes. The result is a two-dimensional image for each of the three wire planes, where the two dimensions are wire number and time. These 2D hits are used as inputs to the Pandora Software Development Kit [16]. Pandora contains pattern recognition algorithms that have been optimized to reconstruct tracks from neutrino interactions in liquid argon TPCs at the BNB energy range. The Pandora algorithms take a set of hits and reconstruct neutrino interaction vertices.

At this point the size of each event has been reduced from millions of pixels to about 20 reconstructed track objects with very little information loss. We can attempt to identify the type of particle and interaction that produced the set of tracks. In the NC elastic case, we want to specifically select proton tracks.

#### 4.2. Proton track identification

Neutral-current elastic interactions are the most difficult to detect automatically because there is only one visible particle coming from the interaction vertex. There is no unique topology separating these events from the cosmic background.

Each reconstructed track object in a MicroBooNE event has several reconstructed physics properties associated with it. These properties fall into the categories of geometric, calorimetric, and optical. The geometric properties are related to the position, shape and size of the track. This includes variables like whether the track is entering the TPC, how long the track is, and how curvy a track is. Calorimetric properties all have to do with the charge deposited along the track. We can use information about how much total charge was deposited by the track, the average charge deposited per cm, and the difference between the amount of charge deposited at the beginning or the end of the track. We can also create variables that represent the shape and

scale of the  $dE/dx$  (or  $dQ/dx$ ) curve at any point along the reconstructed track. Additionally, we can use optical information from the PMT system to help characterize tracks. In this work we use the distance between the reconstructed track and the closest optical flash that was in the beam time window.

*4.2.1. Gradient decision tree boosting* To identify proton tracks, we use a gradient-boosted decision tree classifier. We chose to use decision trees because they are easily interpretable and the inputs can be a mix of numeric and categorical variables. Below is a short description of gradient tree boosting. A more detailed description can be found in the documentation for the XGBoost[17] software library that was used.

A decision tree can be thought of as a series of if/else statements that separate a data set into two or more classes. The goal of each cut is to increase the information gain. For numerical variables any cut value can be selected by the tree. At each node of the tree, a split is chosen to maximize information gain until a set level of separation is reached. At the terminus of the series of splits, called a leaf, a class is assigned.

Two weaknesses of decision trees are their tendency to over fit the training data and the fact that the output is a class label and not a probability. Gradient-boosting addresses both of these issues by combining many weak classifiers into a strong one. Each weak classifier is built based on the error of the previous one. For a given training set, whenever a sample is classified incorrectly by a tree, that sample is given a higher importance when the next tree is being created. Mathematically, each tree is training on the gradient of the loss function. After all of the trees have been created, each tree is given a weight based on its ability to classify the training set, and the output of the gradient-boosted decision tree classifier is the probability that a sample is in a given class.

*4.2.2. The decision tree model* We created a multi-class gradient-boosted decision tree classifier, using the XGBoost software library, to separate five different track types: any proton track, muons or pions from BNB neutrino interactions, tracks from electromagnetic showers from BNB interactions, and any non-proton track produced by a cosmic ray interaction. The classifier takes reconstructed track features as input and outputs a probability of the track having been produced by each of the given particle types. The reconstructed features are based on the track's geometric, calorimetric, and optical properties.

The training data that we use to make the decision trees comes from Monte Carlo simulation. The BNB interactions are simulated using the GENIE neutrino generator [18], and cosmic interactions are simulated using the CORSIKA cosmic ray generator [19]. The particles generated by GENIE and CORSIKA are passed to Geant4 [20] where they are propagated through a simulated MicroBooNE detector. For training and testing of the trees we only use tracks that were reconstructed in LArSoft.

Of the reconstructed test tracks that were input to the classifier, 84% of the protons from simulated neutrino interactions, and 63% of the protons from simulated cosmic interactions were classified correctly as protons. Figure 3 shows the protons from simulated neutrino interactions as a function of proton kinetic energy. Of the reconstructed test tracks that were classified as protons, 89% were true simulated protons (22% neutrino induced protons and 67% cosmic induced protons). Figure 4 shows the breakdown of track types that are classified as protons. To maximize efficiency or purity we can require a lower or higher proton probability from the classifier. Figure 5 shows the efficiency versus purity for different proton probability cuts in the range from zero to one.

The decision tree classifier was used on a small sample of MicroBooNE data as a performance check. Figures 6 and 7 show tracks from the data sample that were selected by the classifier as being very likely protons.

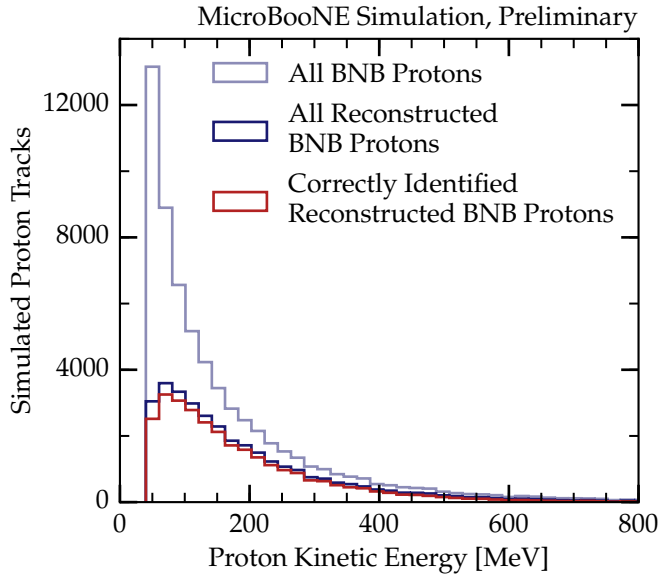


**Figure 3.** Number of simulated proton tracks as a function of true simulated kinetic energy is shown. The light blue line shows the total number of protons from simulated BNB neutrino interactions. The dark blue line shows the total number of those tracks that were reconstructed with the Pandora algorithms. The red line shows the subset of the reconstructed tracks that are classified as protons by the boosted decision trees.

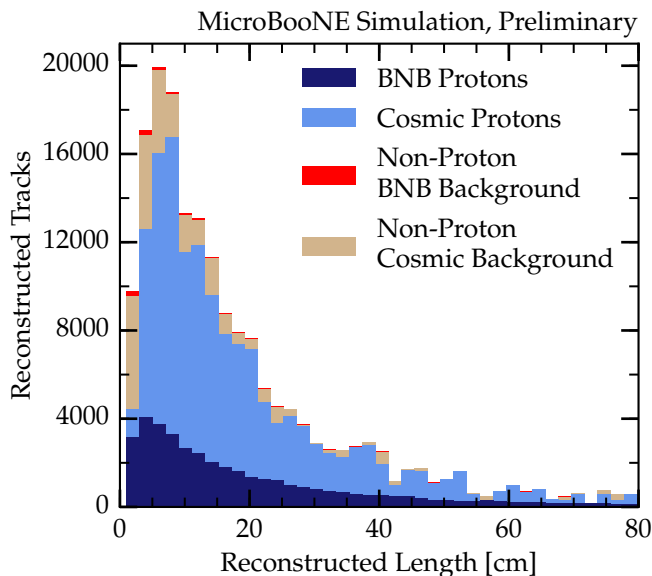


**Figure 4.** Breakdown of the simulated particle types that are classified as protons by the boosted decision trees as a function of reconstructed track length. The blue filled area shows all simulated protons, both cosmic and neutrino-induced, and the dark blue line shows the protons from simulated BNB neutrino interactions. The tan filled area shows all other simulated cosmic tracks that are classified as protons, and the red filled area shows all other tracks from simulated BNB neutrino interactions that are classified as protons.

#### 4.3. NC elastic event selection

So far, we have kept the proton selection general to all interaction types. For NC elastic events, we would use the output of the decision trees along with other event information such as the total number of reconstructed tracks to select the events of interest. This can also be used to select charged-current elastic events with a similar efficiency to use for normalization of the NC elastic cross section. If we are only interested in one specific topology, and do not wish to be general, it is trivial to re-train the classifier using protons from NC elastic interactions as the only positive input and protons from other interactions as a background input.

## 5. Conclusions

Whether the strange quarks in the nucleon sea contribute negatively or not at all to the spin of the nucleon is an open question. Elastic neutrino-proton scattering offers an unique way to determine  $\Delta s$  that is independent of the assumptions required by previous measurements. The

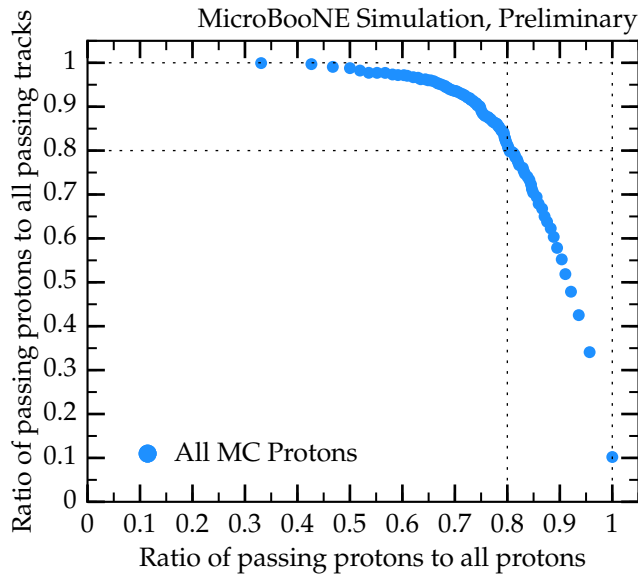


**Figure 5.** The efficiency versus the purity of simulated protons selected by the boosted decision tree classifier for a series of proton probability cuts between zero and one.

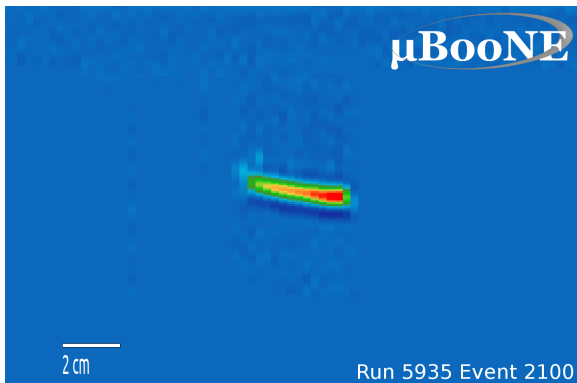


**Figure 6.** Proton track candidate in MicroBooNE data. The track was selected by the decision tree classifier as being very likely a proton.

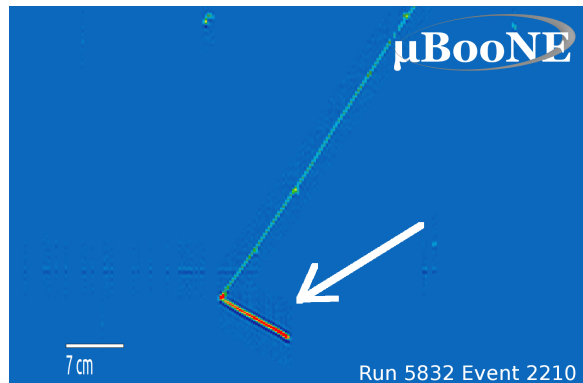


**Figure 7.** Proton track candidate in MicroBooNE data. The white arrow points to a track that was selected by the decision tree classifier as being very likely a proton.

MicroBooNE liquid argon TPC can detect low- $Q^2$  NC elastic events and is currently taking neutrino data at Fermilab. Automated event reconstruction and selection methods are being developed to analyze the large amount of high-resolution neutrino events in MicroBooNE. In these proceeding, we summarize the current status of MicroBooNEs automatic reconstruction and identification of proton tracks in neutral-current and charged-current interactions. The automated reconstruction chain in MicroBooNE successfully reduces the size of the events from millions of pixels to individual reconstructed track objects. This allows us to use boosted decision trees for proton identification. The boosted decision tree we presented here classifies 84% of simulated protons from neutrino interactions correctly and further tuning and improvement of the results is possible.

### Acknowledgments

This work was supported by the US Department of Energy, Office of Science, Medium Energy Nuclear Physics Program.



## References

- [1] Alberico W M, Bilenky S M and Maieron C 2002 *Phys. Rept.* **358** 227–308 (*Preprint hep-ph/0102269*)
- [2] Ashman J *et al.* (European Muon) 1989 *Nucl. Phys.* **B328** 1
- [3] Ellis J and Jaffe R 1974 *Phys. Rev. D* **9**(5) 1444–1446 URL <http://link.aps.org/doi/10.1103/PhysRevD.9.1444>
- [4] Aidala C A, Bass S D, Hasch D and Mallot G K 2013 *Rev. Mod. Phys.* **85** 655–691 (*Preprint 1209.2803*)
- [5] Ahrens L A *et al.* 1987 *Phys. Rev.* **D35** 785
- [6] Garvey G T, Louis W C and White D H 1993 *Phys. Rev. C* **48**(2) 761–765 URL <http://link.aps.org/doi/10.1103/PhysRevC.48.761>
- [7] Aguilar-Arevalo A A *et al.* (MiniBooNE) 2010 *Phys. Rev.* **D82** 092005 (*Preprint 1007.4730*)
- [8] Pate S and Trujillo D 2014 *EPJ Web Conf.* **66** 06018 (*Preprint 1308.5694*)
- [9] Armstrong D S and McKeown R D 2012 *Ann. Rev. Nucl. Part. Sci.* **62** 337–359 (*Preprint 1207.5238*)
- [10] Cates G D, de Jager C W, Riordan S and Wojtsekhowski B 2011 *Phys. Rev. Lett.* **106** 252003 (*Preprint 1103.1808*)
- [11] Patrignani C *et al.* (Particle Data Group) 2016 *Chin. Phys.* **C40** 100001
- [12] Acciarri R *et al.* (MicroBooNE) 2016 *Submitted to: JINST* (*Preprint 1612.05824*)
- [13] The MicroBooNE Collaboration 2016 *MicroBooNE Public Note* **1002**
- [14] Church E D 2013 (*Preprint 1311.6774*)
- [15] The MicroBooNE Collaboration 2016 *MicroBooNE Public Note* **1009**
- [16] The MicroBooNE Collaboration 2016 *MicroBooNE Public Note* **1015**
- [17] Chen T and Guestrin C 2016 *CoRR* (*Preprint 1603.02754*) URL <http://arxiv.org/abs/1603.02754>
- [18] Andreopoulos C *et al.* 2010 *Nucl. Instrum. Meth.* **A614** 87–104 (*Preprint 0905.2517*)
- [19] Heck D, Schatz G, Thouw T, Knapp J and Capdevielle J N 1998
- [20] Agostinelli S *et al.* (GEANT4) 2003 *Nucl. Instrum. Meth.* **A506** 250–303